Demand-side management study for cascade air-water heat pump coupled with thermal energy storage in the UK domestic sector

Khoa X. Le [1], Ming Jun Huang [1], Neil J. Hewitt [1]*

[1] Centre for Sustainable Technologies, University of Ulster, BT37 0QB, United Kingdom
* Corresponding author. Email: le-k@ulster.ac.uk; Tel. +44 (0)289 036 6413

Abstract
Cascade air to water heat pumps (AWHPs), which have better performance and lower compressor ratios than single-stage AWHPs at low ambient temperatures and high outlet water temperature lift, may be a potential retrofit technology for decarbonising space and hot water heating in the UK domestic sector. This is because they can directly replace existing fossil-fueled boilers without the requirement of significant modifications to the heating distribution systems, which can reduce installation costs and disruptions when retrofitting. Also, the coupling of AWHPs and TES along with demand-side management (DSM) is a promising technology to meet the domestic thermal demands with an efficient utilization of grid operation and cost savings for end-users. In this paper, validated building energy simulations of a cascade AWHP and TES applying different DSM strategies are presented. Particularly, three rule-based control approaches based on: 1) dynamic electricity market prices, 2) ambient temperatures, 3) both dynamic market prices and ambient temperatures, were applied to compare their performance with the base case in which the heat pump supplied heat directly to the domestic without using the TES. TRNSYS 17 software was utilised to model and simulate the system performance. Simulation results showed that, while the heat pump controlled with the DSM strategies had lower efficiency than the base case, cost savings were obtained. Although the DSM based on favourable ambient temperatures yielded slightly better efficiency than the one based on dynamic market prices, its running cost was higher. Finally, how the control approaches affected the grid demand and wind energy curtailment is also discussed in the paper.

Keywords: Cascade air-water heat pump; thermal energy storage; demand-side management; dynamic electricity prices; building energy simulation; TRNSYS.

Nomenclature

W	electric input power of the heat pump (kW)
T	temperature (˚C)
t	time (minute)
RH	outdoor relative humidity (%)
PLF	part load factor (-)
PLR	part load ratio (-)
Subscript	
w	water outlet of the heat pump
a	ambient air
def	Defrost
fr	Frost

1 Introduction

Space heating and domestic hot water (DHW) provided by conventional boilers accounted for 78% of domestic energy consumption [1] and 40% of domestic greenhouse gas emissions in the UK [2]. To achieve the binding target of carbon emission reduction up to 80% by 2050 compared to 1900s levels, these energy demands should be decarbonised by replacing fossil-fueled boilers with air-water heat pumps (AWHPs).

While many studies [3-5] attempted to assess the performance of AWHPs when retrofitted into the UK housing stock, most of them were carried out with single-stage low temperature AWHPs (outlet water temperature below 55°C) equipped with under-floor heating and/or oversized/advanced radiators. Replacing conventional boilers with these heat pump systems is more likely to increase installation costs because the existing heating distribution systems need to be modified to allow these heat pumps to work efficiently. Cascade AWHPs (CAWHPs), employing two vapor compression cycles, can be a potential alternative heating source for retrofitting the UK built environment. This is because CAWHPs can provide high water flow temperatures (over 65°C), similar to the outlets of fossil-fueled boilers, with better performance and lower compressor ratios compared to low temperature AWHPs. Therefore, they can help to prevent significant modifications to the heating distribution systems, which results in low installation costs when retrofitting. Although CAWHPs are high energy efficient equipment, electricity demanding during the high peak operation is an issue for the grid.

In the UK, renewable power generation (especially wind energy) has increased, but the mismatch between electricity supply and demand has posed challenges for grid operation efficiency. Thermal energy storage (TES) combined with heat pumps has significant merits for demand-side management (DSM) that is a promising technology to address this issue. Also, such integrated systems can shift the electrical demands from peak-load to low-load periods, which can help to balance the grid and reduce electricity bills for homeowners while guaranteeing thermal comfort. Due to the merits that

DSM of heat pumps with TES can bring to the built environment, there is much research in literature focusing on this technology. However, little attention has been paid to the DSM of CAWHPs with TES at the domestic level.

Rule-based control DSM of heat pumps with TES using variable electricity market prices is a popular simple approach to obtain benefits for the power system and cost savings for end-users while guaranteeing thermal comfort, as dynamic electricity prices reflect the grid and renewable energy situations. Nevertheless, controlling AWHPs based on dynamic market prices might induce reduced heat pump efficiency because the heat pumps tend to operate during night time where ambient temperatures are lower [6]. Whilst this issue has been carried out in the previous studies [7-8], there is little information about the comparison between DSM controlled based on dynamic market prices and favourable ambient temperatures aiming at increasing system efficiency.

In this paper, the analysis of DSM of a CAWHP coupled with TES in a UK residential building is presented. Different rule-based control approaches based on dynamic electricity market prices and variable ambient temperatures were carried to compare their performance. A base case scenario in which the TES was not operated was also introduced as a reference to make the comparison. TRNSYS 17 software [9] was used to model and simulate the investigated system along with the designed DSM strategies, which has been validated against the measurement results in the previous studies [10-11].

2 System description

Schematic of the system investigated in this study is shown in Figure 1. The house was a mid-terraced "hard-to-heat" dwelling built under the 1900s specifications. The building had two floors in which the first floor was living spaces with kitchen, while bed rooms and bathroom were located at the second floor. The heat pump was a variable capacity CAWHP that employed two vapor compression cycles, and this heat pump was a commercially available unit. The storage was a sensible water thermal energy tank. Main characteristics of the system can be seen in Table 1.

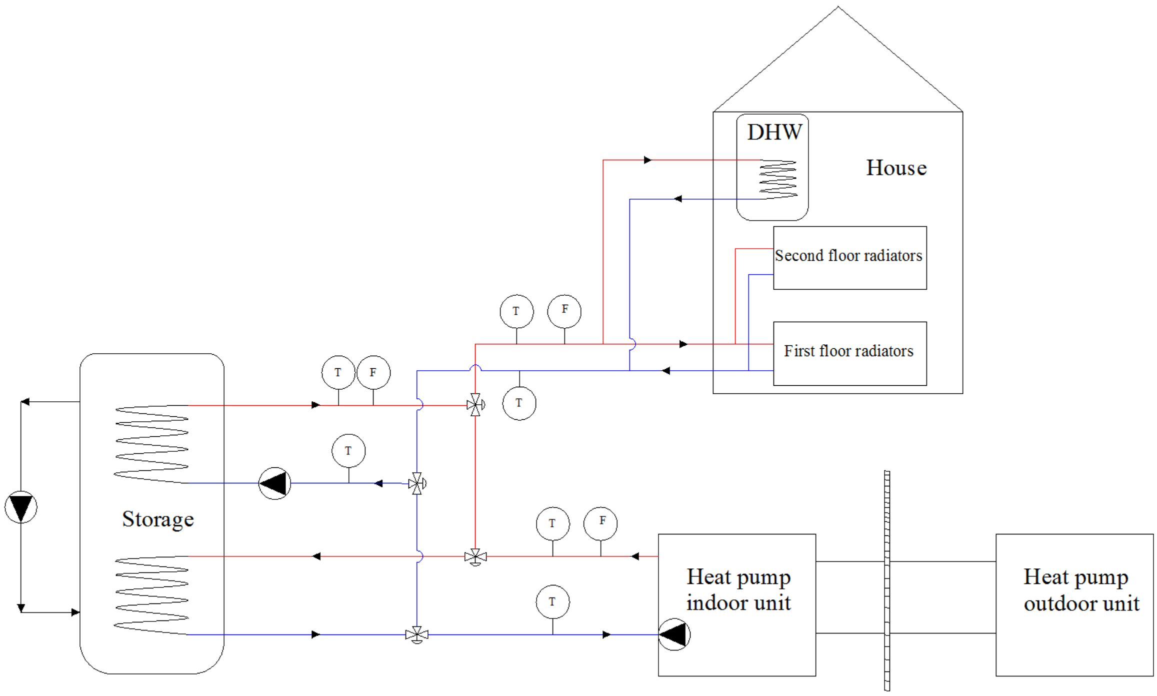

Figure 1: Schematic of the investigated CAWHP domestic heating system with the TES.

Table 1: Main characteristics of the house and the heating system.

		Value	Unit
House	Location	Belfast, Northern Ireland, UK	-
	Number of occupants	Three	-
	Ground floor heated area	110	m^3
	First floor heated area	150	m^3
	U-value of external walls	1.65	W/m^2K
	U-value of roof	1.42	W/m^2K
	U-value of floor	0.67	W/m^2K
	U-value of windows	4.8	W/m^2K
	U-value of doors	0.422	W/m^2K
	Infiltration rate	1.15	ACH
Heat Pump	Working fluids	R-410A (outdoor unit) and R-134a (indoor unit)	-
	Nominal COP (at 7˚C ambient temperature and 80˚C outlet water temperature)	2.5	-
	Nominal heat capacity (at 7˚C ambient temperature and 80˚C outlet water temperature)	11	kW
Storage tank	Capacity	1	m^3
	Heat loss coefficient	1	W/m^2K
DHW tank	Capacity	0.162	m^3
	Temperature maintained	Between 50 and 60	˚C
	Standing heat loss	2.74	kWh/24hrs

3 Modelling

TRNSYS 17 was utilised to model and simulate the system physicality depicted in Figure 1. The developed models, including house model, CAWHP model and TES model, have been validated against the measurement data, which are mentioned in the previous studies [10-11].

3.1 Heat pump model

The variable capacity CAWHP was modelled using TRNSYS Type 1231 that relied on a characterized performance map comprising of full load and part load curves. The performance map did not account for defrost cycles, so a separate defrost model was developed and incorporated outside the heat pump Type 1231. The empirical expressions used for full load, part load and defrost operation are given in Table 2.

Table 2: Empirical expressions of the heat pump model.

Full load curve	$W = -1.01 + 0.7T_w + 0.24T_a - 0.01T_w^2 + 0.000051T_w^3 - 0.0105T_wT_a + 0.000075T_w^2T_a$
	$COP = -1.797 + 2.133T_w - 0.107T_a - 0.0034T_w^2 + 0.000016T_w^3 + 0.0046T_wT_a - 0.000035T_w^2.T_a$
Part load curve	$PLF = -0.0234PLR^2 + 3.8884PLR - 58.777$
Defrost operation (condition: ambient temperature ≤ 7°C and relative humidity ≥ 65%)	$t_{fr} = 39 - 1.06T_a + 0.33RH + 0.13{T_a}^2 - 0.0093RH^2 - 0.018{T_a}^3 - 0.00006RH^3$
	$t_{def} = 56.2 - 0.34T_a - 3.56t_{fr} - 0.047{T_a}^2 + 0.079t_{fr}^2 + 0.0096{T_a}^3 - 0.00057t_{fr}^3$

3.2 Thermal storage tank model

The TES was modelled using TRNSYS Type 534. The tank was set up with seven nodes and two coiled tube heat exchangers. The heat exchanger for charging the tank occupied in three nodes placed at the tank's bottom, while another for discharging was in the other four nodes. The tank size and heat loss coefficient were set 1 m^3 and 1 W/m^2K, respectively, as it was enough to shift the three-hour thermal demands of the house.

3.3 Whole couple house model and DHW model

The geometry of the building was drawn in Sketchup software and then imported into TRNSYS Type 56. U-values and characteristics of the house were set for the model as mentioned in Table 1. The central heating system and occupancy patterns were assumed to be active identically for both weekdays and weekends (Figure 2), which were obtained from the work of Kelly et al. [12]. In particular, the central heating system was on during the periods of 6am-9am and 4pm-11pm every day to maintain the dining room temperature between 19.5˚C and 21˚C, as well as DHW temperature from 50˚C to 60˚C.

The DHW tank was modelled using TRNSYS Type 534. The collected data of DHW consumption in [13] was utilised as an input profile for the DHW drawing patterns in the model.

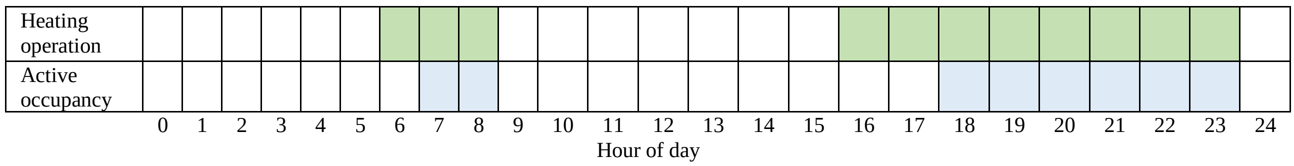

Figure 2: Daily operating hours of central heating system and active occupancy (Data were adapted from [12]).

4 Methodology

4.1 Definition of SMP and ambient temperature percentiles

The DSM strategies in this study were performed based on daily single market price (SMP) percentiles and daily ambient temperature percentiles interchangeably. This means that the operation of the heat pump and the TES was controlled based on the daily rankings of variable electricity market prices or ambient temperatures or both. Examples of SMP and ambient temperatures along with their daily percentiles are shown in Figure 3. It can be seen in the figure that if the SMP or ambient temperature was highest in a day, its percentile was 100%, and vice versa. The historical data of SMP and ambient temperatures were obtained from SEMO (15-minute intervals) [14] and MET Office (one-hour intervals) [15], respectively.

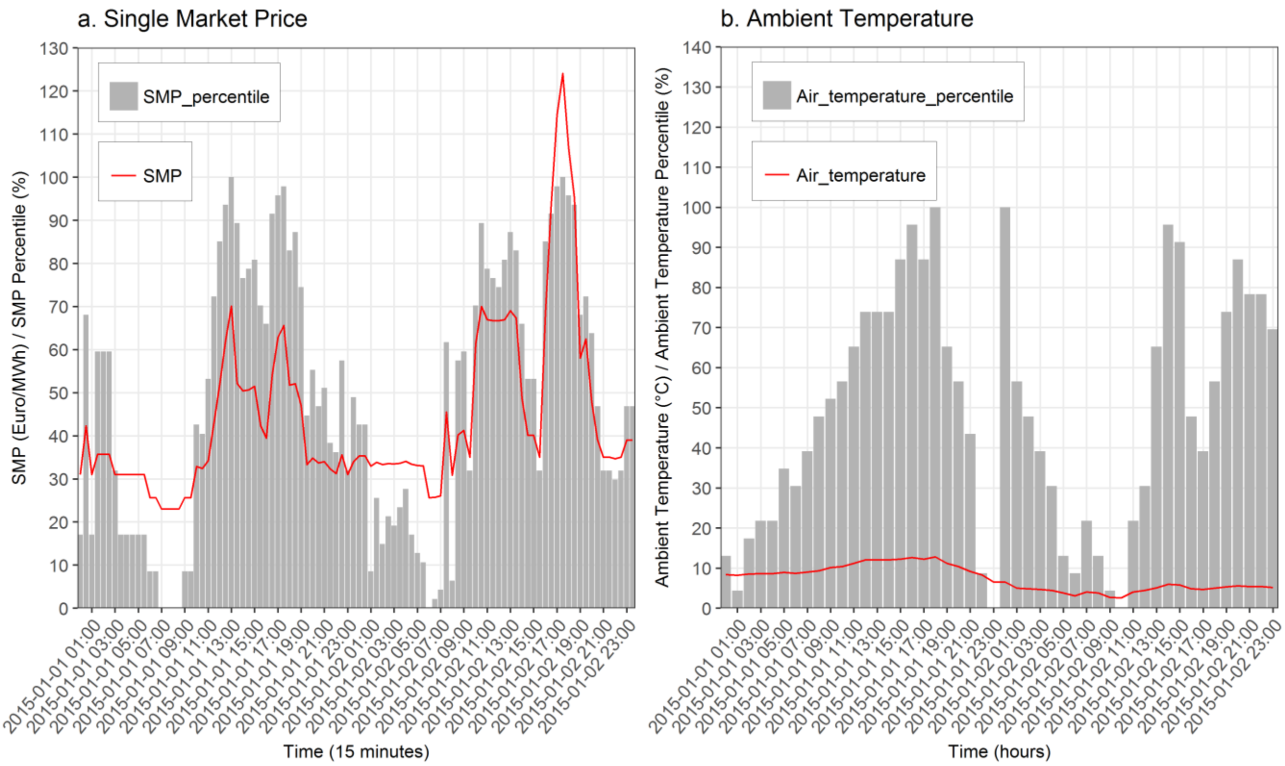

Figure 3: SMP and ambient temperatures and their daily percentiles in two continuous days.

4.2 Simulations

After developing the models, series of simulations with different DSM strategies were undertaken. The simulations were run for a whole year period with the real weather data of Belfast-Northern Ireland from December 2014 to November 2015. Details of the simulations carried out are described as follows.

- **Base Case:** this simulation set was run with the heat pump system operating without the TES. In particular, the heat pump was turned on and off during the daily operating hours of the central heating system to directly satisfy the house heat demands.

- **SMP based:** in this simulation, the TES was used as a DSM tool to decouple the house heat demands during the periods of high electricity prices (daily SMP percentile ≥ 80%), and to store the energy when the electricity prices were low (daily SMP percentile ≤ 20%). Control algorithm of this DSM in each simulation time step can be seen in Figure 4.

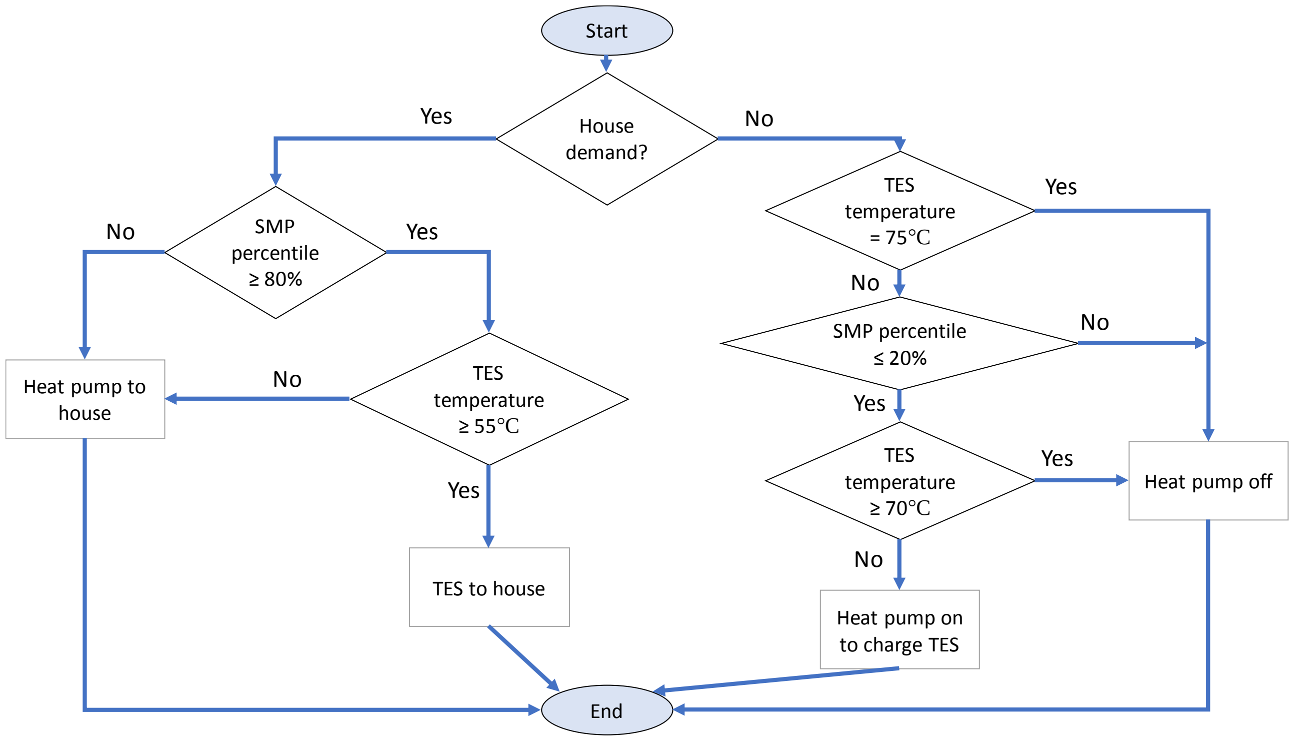

Figure 4: Control algorithm of *SMP based* in each simulation time step.

- **Air temperature based:** The TES in this simulation set was also used to decouple the house heat demands during the time of peak electricity prices, but the heat pump was turned on to charge the TES when external air temperatures were high (daily ambient temperature percentile $\geq$ 80%), which allowed the heat pump to have a good performance. Figure 5 shows how this control strategy was set in the simulation.

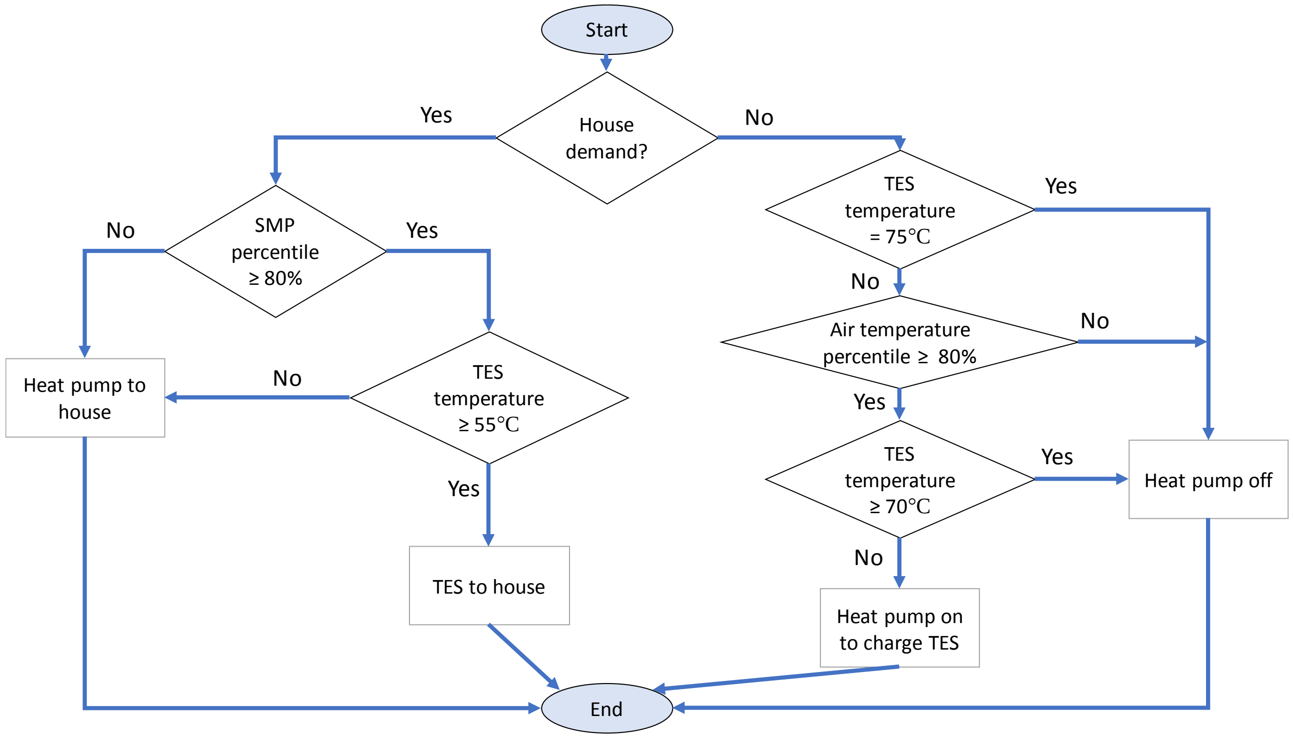

Figure 5: Control algorithm of *Air temperature based* in each simulation time step.

- **SMP and air temperature based:** this DSM was designed to utilise the heat pump to top up the TES when electricity prices were relatively low (SMP percentile $\leq$ 50%) and ambient temperatures were relatively high (ambient temperature percentile $\geq$ 50%). During the periods of high electricity prices (SMP percentile $\geq$ 80%), the TES was also used to decouple the building heat demands. Figure 6 illustrates how this DSM strategy was carried out.

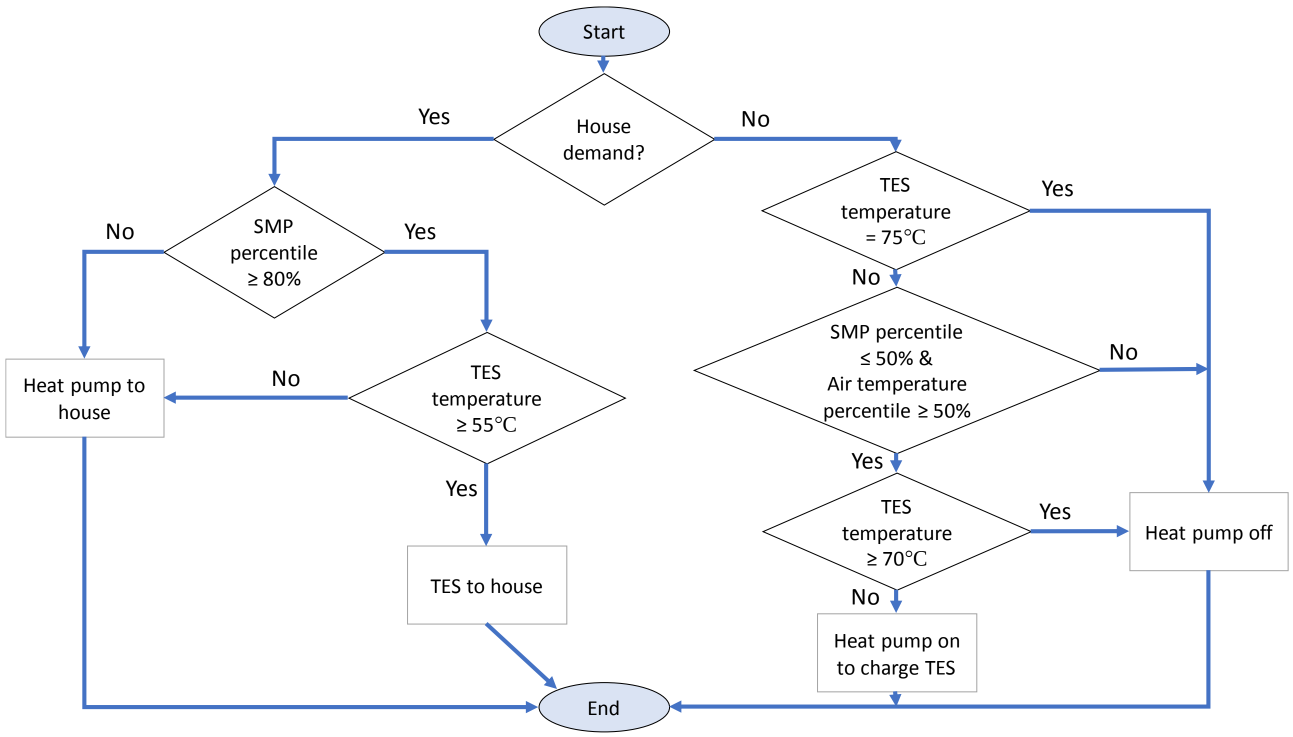

Figure 6: Control algorithm of *SMP and air temperature based* in each simulation time step.

4 Simulation results and discussion

Annual COP of the heat pump is defined as the ratio between the total useful heat output to the house which accounts for the heat losses of the TES and piping, and the total electric consumption throughout the year, as expressed in Equation 1.

$$Annual\ COP\ (-) = \frac{Total\ useful\ heat\ output\ of\ the\ year\ (kWh)}{Total\ electric\ consumption\ of\ the\ year\ \ (kWh)} \qquad (1)$$

4.1 Impact of control strategies on annual performance

Annual simulation results are summarized in Table 3. It can be seen in the table that *Base Case* revealed the highest annual COP (2.26), while *SMP based* yielded the lowest efficiency (annual COP of 1.88). Also, efficiency of the heat pump in *Air temperature based* (annual COP of 1.91) was just slightly better those of *SMP based* as well as *SMP and air temperature based*.

Table 3: Yearly results of four simulations.

	Base Case	**SMP based**	**Air temperature based**	**SMP and air temperature based**
Annual COP [-]	2.26	1.88	1.91	1.89
Electric use [kWh]	6645	10910	10746	10845
Useful heat output [kWh]	15008	20464	20503	20474
Running cost [Euro]	581	492	526	505

In Figure 7, the power consumption of the heat pump throughout the year in each control strategy is depicted to compare its operation patterns. The heat pump controlled based on SMP percentiles tended to charge the TES during night time where the electricity prices were low (Figure 7b), while the one controlled based on ambient temperature percentiles tended to top up the TES during day time (Figure 7c) where external air temperatures were favourable. Also, the heat pump in *SMP based* tended to charge the TES at night where ambient temperatures were normally lower than daytime, leading to the reason why its COP was slightly lower than the one in *Air temperature based* (Table 3). Looking at Figure 7d, the time of charging the TES was spread in both the early morning and afternoon, but mostly in the afternoon where SMP and ambient conditions were favourable. In short, energy consumption patterns of the heat pump for charging the TES varied diurnally, but there were just small figures of COP difference (maximum of 1.6%) regarding three DSM strategies. The reason for this might come from the small changes of ambient temperatures between day and night of the selected location (Belfast, Northern Ireland), and therefore future study will investigate this issue.

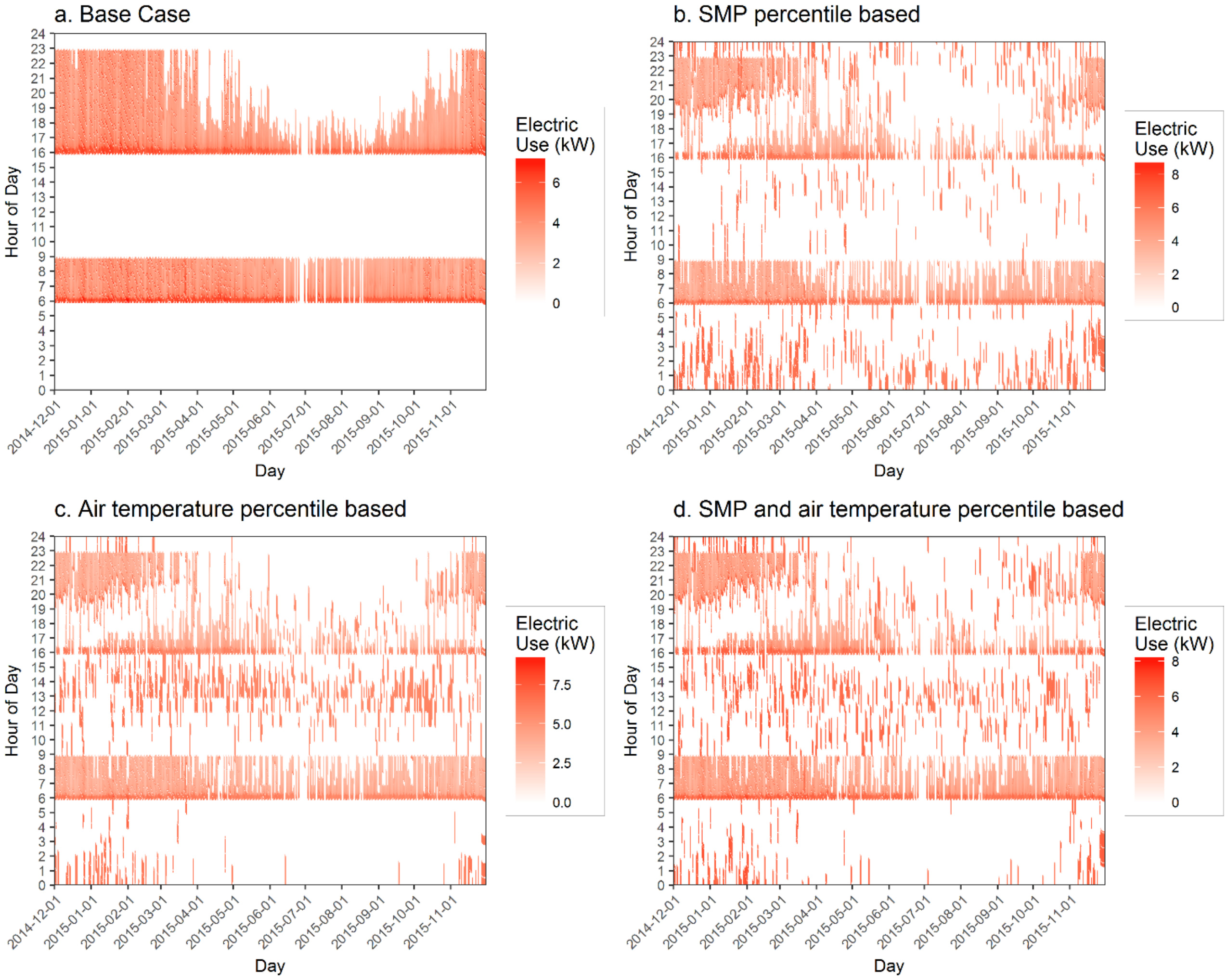

Figure 7: Heat pump electric input power of four control strategies throughout the year (out of the central heating hours (6am-9am and 4pm-11pm) was the operation of charging the TES).

4.2 Impact of control strategies on running costs

In Table 3, as the TES in *Base Case* was not used, its annual operating cost was highest (581 Euro). *SMP based* was lowest (492 Euro), followed by *SMP and air temperature based* (505 Euro) and *Air temperature based* (526 Euro), respectively. Whilst *Air temperature based* was slightly better efficient than *SMP based*, running cost of *Air temperature based* was higher than that of *SMP based*. Furthermore, while *SMP and air temperature based* was introduced to take advantage of both low electricity prices and higher efficiency compared to *SMP based*, it could not obtain cost savings. Thereby, an optimization study should be carried out in the future to seek the better cost benefits of this DSM approach.

4.3 Impact of control strategies on the grid demand

An example of how the different control strategies affected on the grid demand in two continuous days is illustrated in Figure 8. The heat pump demand was aggregated for 5% of the current housing stock in Northern Ireland, the UK (5% of 776526 dwellings [16]).

According to *Base Case* scenario (Figure 8a), the grid demand would be posed a challenge since there was an added peak demand from 4pm to 7pm. In contrast, this peak demand challenge would be mitigated if three control strategies were applied (Figure 8b-d) because the heat pump was shifted to prevent the peak electricity prices which highly coincided with the peak demand periods.

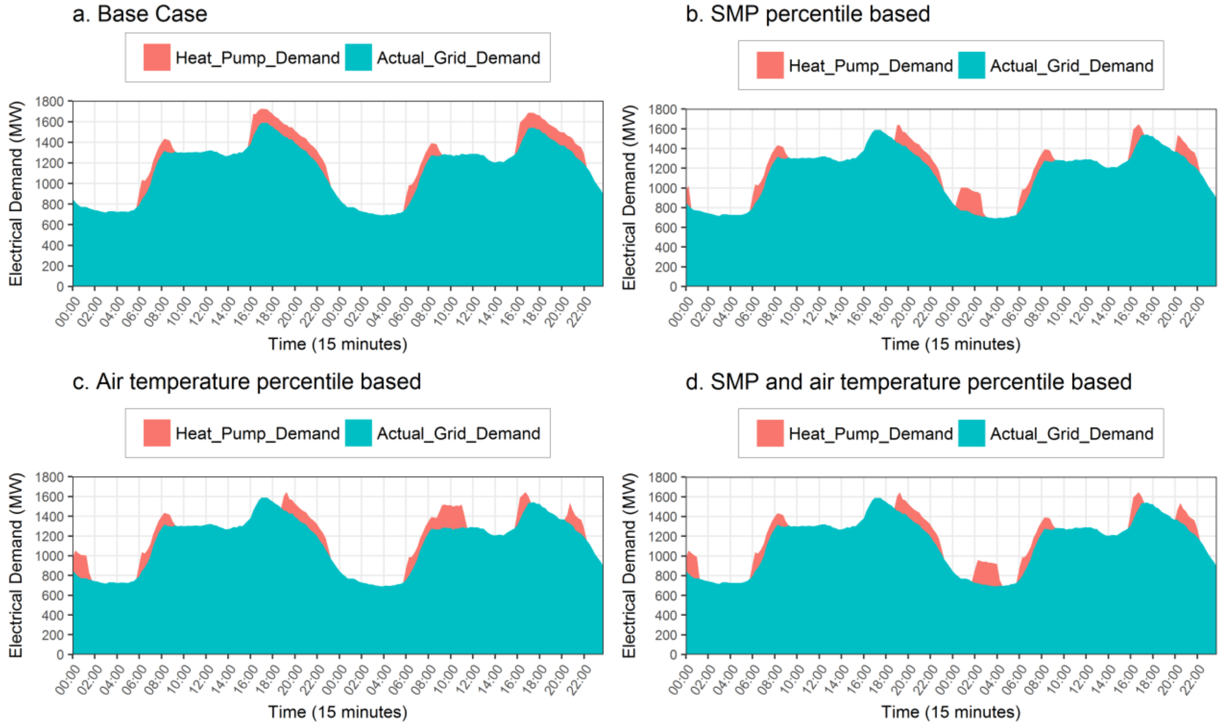

Figure 8: Impact of four control strategies on grid demand in two continuous days (Data of the actual grid demand were obtained from [14]).

4.4 Impact of control strategies on wind curtailment

How much wind energy curtailment could be prevented in Northern Ireland was also considered for the designed DSM strategies. Examples of wind curtailment power and aggregated heat pump demand in two continuous days are depicted in Figure 9 to illustrate how the wind curtailment prevention was calculated. Particularly, if the heat pumps were operated during the time of wind dispatch-down, it was assumed that wind energy would be used by the heat pumps. In Table 4, the highest figure of prevented wind curtailment was of *Air temperature based* (7.86%/30832 MWh), followed by *SMP and air temperature based* (7.5%/29416 MWh), *SMP based* (7.45%/29244 MWh), and *Base Case* (6.9%/27096 MWh), respectively. In short, while *Air temperature based* did not have better cost savings compared to the other DSM strategies, it could allow more proportions of wind energy to be integrated into the grid.

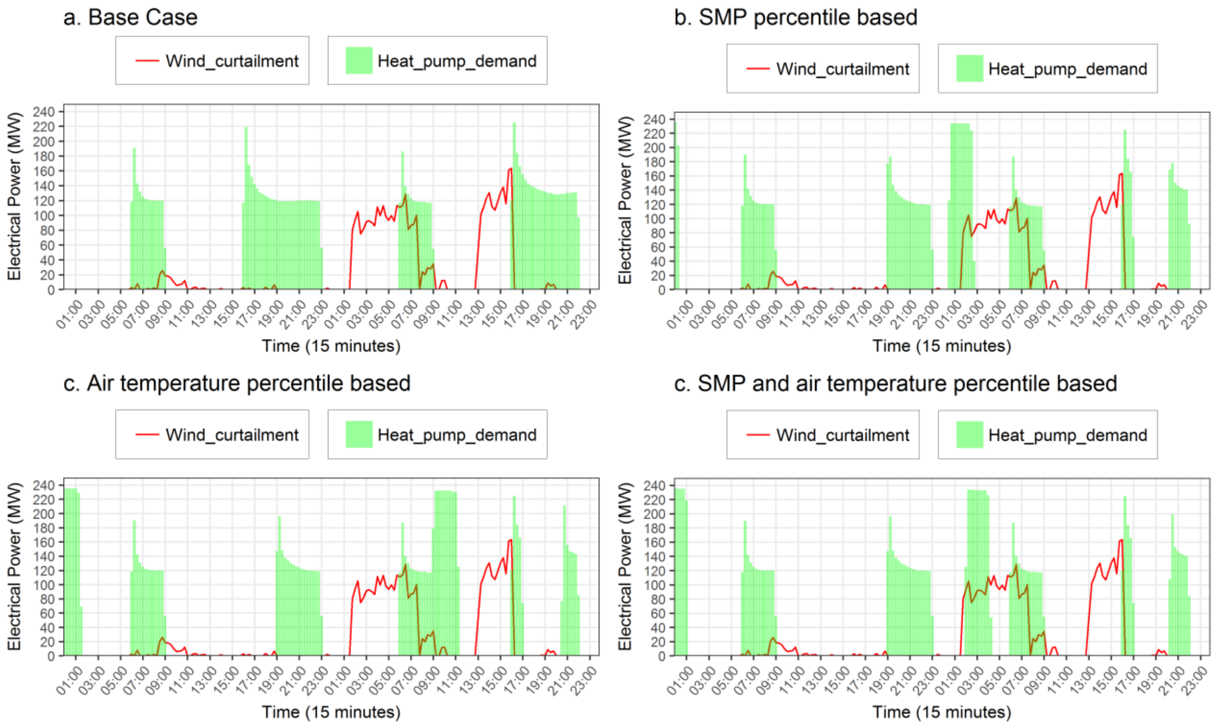

Figure 9: Impact of four control strategies on wind curtailment in two continuous days (Data of the wind curtailment power were obtained from [14]).

Table 4: Comparison of annual wind curtailment prevention (heat pump demand was aggregated for 5% of total dwellings in Northern Ireland).

	Base Case	SMP based	Air temperature based	SMP and air temperature based
Wind curtailment prevention [MWh]	27096	29244	30832	29416
Percentage of wind curtailment prevention [%]	6.9	7.45	7.86	7.5

5 Conclusions

This study investigated the varied DSM strategies for the system of a CAWHP and TES in a UK residential building. The DSM strategies were designed to top up the TES based on daily rankings of dynamic electricity prices or ambient temperatures or both, and to decouple house heat demands during the periods of high electricity prices. After simulating the system with the designed DSM in TRNSYS environment, the results showed that:

- Charging the TES based on the electricity prices had better cost savings, but slightly lower efficiency compared to the one based on ambient temperatures.
- All the DSM strategies could obtain cost savings, the better grid demand performance and the higher figures of prevented wind energy curtailment, compared to the Base Case in which the TES was not used.
- While the air temperature-based DSM did not allow the homeowners to save the costs compared with the electricity-based, more proportions of wind energy could be allowed to the grid associated with the air temperature-based.

The control algorithm based on both electricity prices and ambient temperatures did not have good cost savings, while it was designed to take advantage of low prices and high efficiency. Future research will concern the optimization of this approach. Also, there was not much COP difference between the designed DSM strategies, so future work will investigate this issue. Finally, how storage tank sizing and different storage types (i.e. phase change material) affect the performance of the designed DSM strategies will be carried out in the future work.

Acknowledgements

The study leading to these results has been funded by Research Councils UK (RCUK) under i-STUTE EPSRC project, INTERREG VA SPIRE 2 and H2020, CHESS-SETUP.

References

1. DECC, 2015. Digest of United Kingdom Energy Statistics 2015, Available at: https://www.gov.uk/government/publications/digest-of-united-kingdom-energy-statistics-dukes-2013-printed-version-excluding-cover-pages [Accessed February 20, 2019].
2. DECC, 2012. Emission from Heat: Statistical Summary. Available at: https://www.gov.uk/government/statistics/uk-emissions-from-heat [Accessed February 20, 2019].
3. N. Kelly, J. Cockroft, Analysis of retrofit air source heat pump performance: Results from detailed simulations and comparison to field trial data, Energy and Buildings 43 (1) (2011) 239-245.
4. L. Cabrol, P. Rowley, Towards low carbon homes - a simulation analysis of building-integrated air-source heat pump systems, Energy and Buildings 48 (2012) 127-136.
5. Detailed analysis from the first phase of the Energy Saving Trust's heat pump field trial 2012, Tech. rep., Department of Energy and Climate Change. Available at: https://www.gov.uk/government/publications/greenhouse-gas-reporting-conversion-factors-2018 [Accessed February 20, 2019].
6. D. Fischer, H. Madani, On heat pumps in smart grids: A review, Renewable and Sustainable Energy Reviews 70 (2017) 342–357.
7. D. Fischer, T. Rivera Toral, K. B. Lindberg, B. Wille-Haussmann, H. Madani, Investigation of thermal storage operation strategies with heat pumps in German multi family houses, Energy Procedia 58 (2014) 137–144.
8. J.J. Guo, J.Y. Wu, R.Z. Wang, S. Li, Experimental research and operation optimization of an air-source heat pump water heater, Applied Energy 88 (2011) 4128–4138.
9. TRNSYS 17, a TRaNsient SYstem Simulation program - vol. 3- Component Library Overview, Available at: http://www.trnsys.com/assets/docs/03-ComponentLibraryOverview.pdf [Accessed February 20, 2019].
10. K. X. Le, N. Shah, M. J. Huang, N. J. Hewitt, High temperature air source heat pump and thermal energy storage: Validation of TRNSYS models, Proceedings of the World Congress on Engineering and Computer Science 2017 Vol II WCECS 2017, October 25-27, 2017, San Francisco, USA. Available at: http://www.iaeng.org/publication/WCECS2017/WCECS2017_pp754-759.pdf
11. K. X. Le, M. J. Huang, N. J. Hewitt, Domestic High Temperature Air Source Heat Pump: Performance Analysis Using TRNSYS Simulations, International High Performance Buildings Conference at Purdue, July 9-12, 2018, Paper 315, Available at: https://docs.lib.purdue.edu/ihpbc/315/

12. N. Kelly, Paul G. Tuohy, Adam D. Hawkes, Performance assessment of tariff-based air source heat pump load shifting in a UK detached dwelling featuring phase change-enhanced buffering, Applied Thermal Engineering 71 (2014) 809-820.
13. N. N. Shah, C. Wilson, M. J. Huang, N. J. Hewitt, Analysis on field trial of high temperature heat pump integrated with thermal energy storage in domestic retrofit installation, Applied Thermal Engineering 143 (2018) 650-659.
14. SEMO, Single Electricity Market Operator, Available at: http://lg.sem-o.com/Pages/default.aspx [Accessed February 20, 2019].
15. MET Office, Available at: https://www.metoffice.gov.uk/weather/forecast/gcey94cuf#?date=2019-02-20 [Accessed February 20, 2019].
16. National Statistics, 2017. The Northern Ireland House Condition Survey. Available at: https://www.nihe.gov.uk/nihcs_2016_preliminary_report.pdf [Accessed February 20, 2019].